Int. J. Nanosci. Nanotechnol., Vol. 16, No. 4, Dec. 2020, pp. 233-241

Improving the Dielectric Properties of the $Ba(Zr_{0.1}Ti_{0.9})O_3$-based Ceramics by Adding a Li_2O–SiO_2 Sintering Agent Step by Step

Rong Ma[1,*], Bin Cui[2], Dengwei Hu[1], Yan Wang[1], Weiwei Zhao[1] and Meijuan Tian[1]

[1]Faculty of Chemistry and Chemical Engineering, Engineering Research Center of Advanced Ferroelectric Functional Materials, Key Laboratory of Phytochemistry of Shaanxi Province, Baoji University of Arts and Sciences, P.O.Box 721013, Baoji, People's Republic of China.
[2]Faculty of Chemistry and Materials Science, Northwest University, P.O.Box 710127, Xi'an, People's Republic of China.

(*) Corresponding author: marong20@126.com.
(Received: 12 February 2020 and Accepted: 12 April 2020)

Abstract

To meet the needs of future multilayer ceramic capacitors (MLCCs), a low sintering temperature, higher capacitance and thinner dielectric layers are necessary. To achieve this goal, an appropriate sintering agent and appropriate doping technique must be developed to reduce the sintering temperature and optimize the ceramic's microstructure. In this study, we researched the effect of Li_2O-SiO_2 (Li-Si-O) and how it is added on the dielectric properties of the $Ba(Zr_{0.1}Ti_{0.9})O_3$-based ceramics. The dielectric constant increased significantly by adding Li-Si-O step by step, but decreased with addition in a one-step. The dielectric constant increased first and then decreased with the increasing of Li-Si-O content, and reached a maximum of 18942 at 0.10 wt% Li-Si-O, and the temperature-capacitance characteristic (TCC) of the samples with a Li-Si-O content less than 0.20 wt% met the Y5V standards. The Li-Si-O reduced the sintering temperature of the $Ba(Zr_{0.1}Ti_{0.9})O_3$-based ceramics to 1100 °C, and the dielectric constant first increased and then decreased with increasing sintering temperature increasing.

Keywords: *Li-Si-O, Step by step method, Dielectric properties, Sintering temperature.*

1. INRODUCTION

There is a growing demand for MLCCs due to the rapid development of surface-mount technology and growing need for portable equipment in the electronics industry [1]. The main development trend for MLCCs is toward higher capacitance, smaller size, and lower cost. The properties of Y5V ceramics are defined by the Electronic Industries Alliance; the "Y" denotes a low temperature limit of -30 °C, the "5" denotes a high temperature limit of 85 °C, and the "V" denotes an allowable capacitance variation range from +22% to -82%. These ceramics are of increasing importance to the rapidly growing electronics industry owing to their good dielectric properties over a wide temperature range and their high permittivity [2,3]. $BaTiO_3$-based ceramics have shown high potential for Y5V ceramics, but $BaTiO_3$-based ceramics are generally sintered at 1350 °C to obtain sufficiently, dense materials, and a noble metal such as Pd must be used as the internal electrodes at that temperature. To reduce the production cost, a suitable sintering agent is usually added to reduce the sintering temperature of the ceramics and to allow the possibility of using a base metal such as Ni as an internal electrode [4,5]. The sintering temperature of $(Ba,Sr)TiO_3$ thin films was reduced from 1350 °C to 900 °C by doping with Li, indicating that the Li was prone to form a liquid phase during sintering [6]. Li ions are also an important liquid sintering additive for $BaTiO_3$ ceramics. Li_2O–SiO_2 has a low melting point and can form a

eutectic mixture in a proper ratio, they could form a eutectic mixture at about 900°C [7]. This suggests that they can easily form a liquid phase and promote the densification of ceramics at a low sintering temperature [8].

To date, the traditional solid-state method has been commonly used to prepare nonhomogeneously doped Y5V-type ceramics [9]. Wang et al. [10,11] used Sm or Yb to modify barium zirconium titanate and developed a Y5V-type dielectric material with a room temperature dielectric constant greater than 23,000 using a traditional multi-step solid phase method, but the homogeneity of the powders was poor. Wang et al. [12] synthesized $Ba(Zr_{0.1}Ti_{0.9})O_3$-Zn-Nb ceramics by means of a sol-gel process with a maximum dielectric constant (ε_{max}) greater higher than 20,000. As an alternative to these previous methods, researchers have used wet chemical routes, such as precipitation method [13], hydrothermal method [14], and sol-gel process [15,16], to prepare $BaTiO_3$-based nanopowders. Unfortunately, the nanopowders used as Y5V-type precursors have complicated compositions, and the first two methods require a washing step that is difficult to control at a production scale. In contrast, the sol-gel process does not require this step and easier to control. This approach also permitted the use of a relatively low-temperature process that avoids contaminating the materials and offers better sintering performance than that of the traditional solid-state method [17]. Therefore, it's necessary to develop an appropriate method is significant to prepare Y5V ceramics with a high dielectric constant and a low sintering temperature.

In the present study, we prepared Li-Si-O doped $Ba_{0.9}Zr_{0.1}TiO_3$-based ceramics with high permittivity and good temperature stability that are capable of meeting the current demand for Y5V-type MLCCs to support device miniaturization in the electronics industry. We also compared the effect of the sintering agent content and how it was added on the dielectric properties of the ceramics.

2. EXPERIMENTAL PROCEDURES

2.1. Synthesis

Synthesis of $Ba(Zr_{0.1}Ti_{0.9})O_3$-based nanopowders using a Li-Si-O sintering agent by the one-step method: we synthesized $Ba(Zr_{0.1}Ti_{0.9})O_3$ nanopowders modified with Cu, Nb, Zn, Mn, and Ce dopants element using the sol-gel process. The precursor reagents were $Ba(CH_3COO)_2$, $Ti(C_4H_9O)_4$, $Zr(NO_3)_4{\cdot}5H_2O$, $Zn(CH_3COO)_2{\cdot}2H_2O$, $Ce(NO_3)_3{\cdot}6H_2O$, $Cu(CH_3COO)_2{\cdot}H_2O$ and $Mn(CH_3COO)_2{\cdot}4H_2O$ and they were all analytical-grade chemicals (with a minimum purity of 99%) obtained from the Shanghai Chemical Reagent Factory (Shanghai, China). $H_3[Nb(O_2)_4]$ solutions were prepared according to the method reported by Das and Pramanik [18]. The overall procedure for the synthesis of the $Ba(Zr_{0.1}Ti_{0.9})O_3$-based nanopowders was as follows: we dissolved a stoichiometric quantity of $Ti(C_4H_9O)_4$ was dissolved in a mixture of absolute ethanol (10 mL) and acetic acid (15 mL), with constant stirring using a magnetic stirrer for 1 h at room temperature to form a uniform $Ti(C_4H_9O)_4$ solution. Next, $Zr(NO_3)_4{\cdot}5H_2O$, $Zn(CH_3COO)_2{\cdot}2H_2O$, $Ce(NO_3)_3{\cdot}6H_2O$, $Cu(CH_3COO)_2{\cdot}H_2O$, $Mn(CH_3COO)_2{\cdot}4H_2O$, $Ba(CH_3COO)_2$, $H_3[Nb(O_2)_4]$, $Si(OC_2H_5)_4$ and CH_3COOLi were dissolved in deionized water (50 mL). Finally, the freshly prepared solutions were slowly added into the above mentioned $Ti(C_4H_9O)_4$ solution and stirred vigorously for 2 h at room temperature to form a homogeneous transparent sol. Gelling was performed on the resulting transparent sol for 40 min in a water bath at 60 °C, followed by aging for 12 h. The xerogels acquired after this step were then dried at 80 °C for 12 h. The xerogels were calcined at 900 °C for 2 h to produce the $Ba(Zr_{0.1}Ti_{0.9})O_3$-based nanopowders.

Synthesis of the Li-Si-O nanocomposite: we weighed a certain amount of $Si(OC_2H_5)_4$ and CH_3COOLi at a ratio of 2 Li to 1 Si. We then mixed the $Si(OC_2H_5)_4$ with C_2H_5OH to get solution A, and added the CH_3COOLi solution to solution A drop by drop, with continuous stirring, to obtain a transparent sol. The sol was aged for 12 h, and dried for 8 h at 80 °C, then the dry Li-Si-O nanocomposite was obtained after calcining at 600 °C for 2 h.

Synthesis of $Ba(Zr_{0.1}Ti_{0.9})O_3$-based nanopowders by adding Li-Si-O nanocomposite by the step-by-step method: we prepared the $Ba(Zr_{0.1}Ti_{0.9})O_3$-based nanopowders by the sol-gel method described earlier in this section, then mixed the $Ba(Zr_{0.1}Ti_{0.9})O_3$-based nanopowders and Li-Si-O nanocomposite (at Li-Si-O rates ranging from 0.0 to 0.8 wt%) by ball milling.

Preparation of the ceramics: the nanopowders were then compressed into pellets (8 mm in diameter and 6 mm in thickness) under a uniaxial pressure of about 6 MPa. These pellets were sintered in air at 1100 °C for 2 h. Finally, the sintered discs were polished, and a silver paste was applied to both sides of each disc for the dielectric measurements.

2.2. Characterization

The phase identification was performed by means of X-ray diffraction measurements (XRD; D8 Advance, Bruker, Frankfurt, Germany) at room temperature using Cu Ka radiation (1.54059 Å). The morphology of the ceramic samples was characterized using a field-emission scanning electron microscope (FE-SEM; Model JSM-5800, JEOL, Tokyo, Japan). Dielectric properties were measured using an LCR meter (Model HP4284A, Hewlett-Packard Company, Santa Clara, California, USA) controlled by a computer. The testing temperature was controlled between 60 °C and 150 °C under test conditions of 1 kHz and 1 Vrms, with a heating rate of 2 °C/min.

3. RESULTS AND DISCUSSION

3.1. Effect of the Addition Way of Li-Si-O on the Phase Composition, Microstructure and Dielectric Properties of the $Ba(Zr_{0.1}Ti_{0.9})O_3$-Based Y5V Ceramic

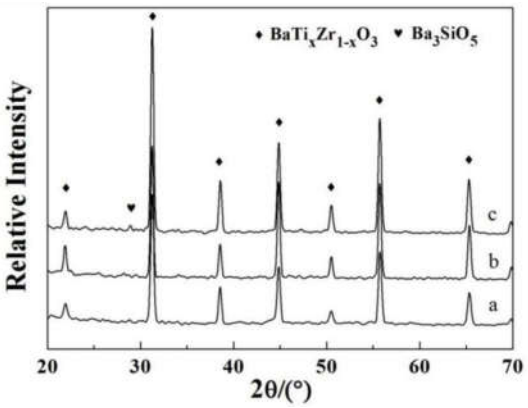

Figure 1. *XRD patterns for the $Ba(Zr_{0.1}Ti_{0.9})O_3$-based ceramics with different methods of Li-Si-O doping: (a) Li-Si-O-free; (b) step by step doping; (c) one-step doping.*

Figure 1 shows the XRD patterns of the $Ba(Zr_{0.1}Ti_{0.9})O_3$-based ceramics with different Li-Si-O doping way. All samples had a cubic perovskite structure indexed based on JCPDS file number 31-0174. No obvious second phase was present when the Li-Si-O was added step by step. However, Ba_3SiO_5 appeared when the Li-Si-O was added in one step. That may because the excess Si ions easily enter into the lattice of $Ba(Zr_{0.1}Ti_{0.9})O_3$, where they produce a secondary phase Ba_3SiO_5 when the Li-Si-O is added in one step; in contrast, the Li-Si-O remains amorphous at the grain boundary when it is added step by step [19].

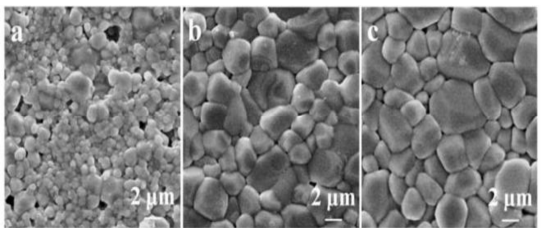

Figure 2. *SEM images of the $Ba(Zr_{0.1}Ti_{0.9})O_3$-based ceramics with different methods of Li-Si-O doping: (a) Li-Si-O-free; (b) step by step doping; (c) one-step doping.*

Figure 2 shows the SEM images of the $Ba(Zr_{0.1}Ti_{0.9})O_3$-based ceramics created using the different Li-Si-O doping methods. The grain size of the ceramics prepared by both methods increased compared to the ceramic without Li-Si-O. This probably resulted from the formation of a liquid Li-Si-O liquid phase during the sintering process, which promoted the process of dissolution and precipitation, thereby making the grains grow [20,21]. The ceramics prepared by adding the Li-Si-O step-by-step were denser than those prepared with one-step addition, and their grain size (about 2.5 μm, Table 1) was smaller than the grain size achieved with one-step addition (about 3.1 μm, Table 1). This may be because more Li-Si-O can inhibit grain growth at the grain boundary. However, more Li and Si ions can enter into the lattice of $BaTiO_3$ with one-step addition, thereby producing a secondary phase that reduced densification of the ceramics.

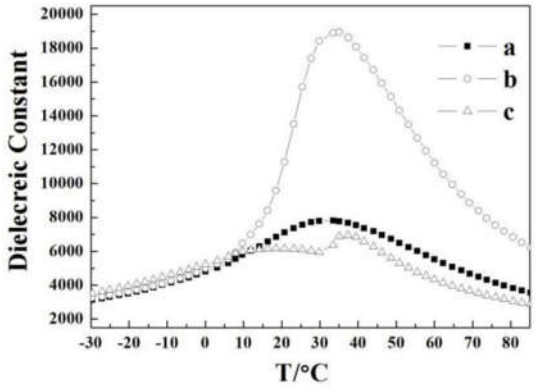

Figure 3. *Temperature dependence of the dielectric constant: (a) Li-Si-O-free; (b) step-by-step doping; (c) one-step doping.*

Figure 3 shows the temperature dependence of the dielectric constant of the ceramics created with different methods of Li-Si-O doping over a temperature range from -30 °C to 85 °C. The maximum dielectric constant (ε_{max}) and dielectric constant at room temperature (ε_r) of these samples are listed in Table 1. The results indicated that doping Li-Si-O step by step can significantly improve the dielectric properties of the $Ba(Zr_{0.1}Ti_{0.9})O_3$-based ceramics, whereas the one-step doping degraded the dielectric properties. This may be due to Li-Si-O staying at the grain boundary during sintering process to form a liquid phase by the step by step doping. Early in the sintering process, the Li-Si-O played the role of sintering agent, whereas late in the sintering phase, it played a modified role [22], which is conducive to the preparation of dense ceramics, thereby significantly improving the dielectric properties of the ceramics. However, with one-step doping, the sintering agent entered into the lattice, changing the distribution of doping ions in the original powder, and instead of improving the density, it degraded the dielectric properties of the ceramic. Therefore, the choice of how to add the sintering agent doping way is significant.

3.2 Effect of Content of the Li-Si-O on the Phase Composition, Microstructure and Dielectric Properties of the $Ba(Zr_{0.1}Ti_{0.9})O_3$-Based Y5V Ceramic

Figure 4 shows the XRD patterns of the $Ba(Zr_{0.1}Ti_{0.9})O_3$-based ceramics with different Li-Si-O contents added step by step. Regardless of the Li-Si-O amounts, the main phase of all the $Ba(Zr_{0.1}Ti_{0.9})O_3$-based ceramics was a perovskite phase. The peaks for the tetragonal-phase in the XRD were indexed based on JCPDS file number 05-0626. Small amounts of Ba_3SiO_5 and Li_8ZrO_6 phases appeared when the Li-Si-O content was 0.6 wt% or higher, which may be due to the development of a rich Li and Si ions phase in the molten glass accumulating at the grain boundaries of the $Ba(Zr_{0.1}Ti_{0.9})O_3$ ceramics; that phase participated in the migration of the grain boundary and

vacancy diffusion that occurred at the grain boundaries, thereby producing a secondary phase [23].

Table 1. *Performance parameters of the ceramics produced by different Li-Si-O doping methods. ε_{max}, maximum dielectric constant; ε_r, room-temperature dielectric constant.*

Li-Si-O doping method	Density (g/cm^3)	ε_{max}	ε_r (25°C)	Average grain size (μm)
Non-doping	5.267	7818	7560	1.8
step by step doping	5.909	18942	18897	2.5
one-step doping	5.454	6173	6107	3.1

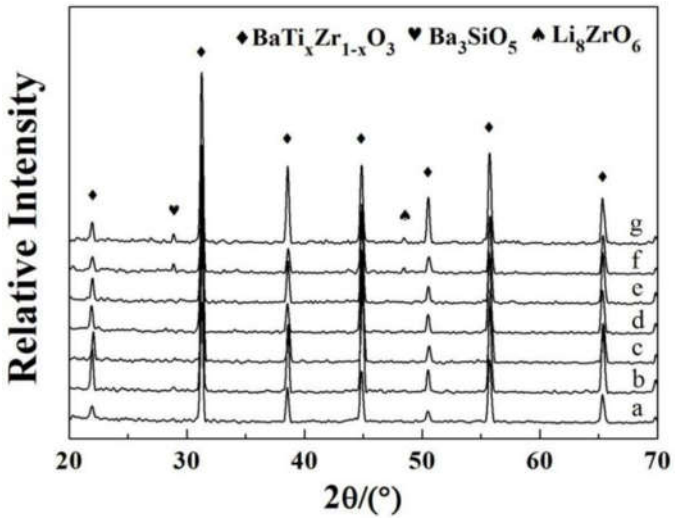

Figure 4. *XRD patterns of the $Ba(Zr_{0.1}Ti_{0.9})O_3$-based ceramics with different Li-Si-O contents: (a) 0 wt%; (b) 0.04 wt%; (c) 0.08 wt%; (d) 0.10 wt%; (e) 0.20 wt%; (f) 0.60 wt%; (g) 0.80 wt%.*

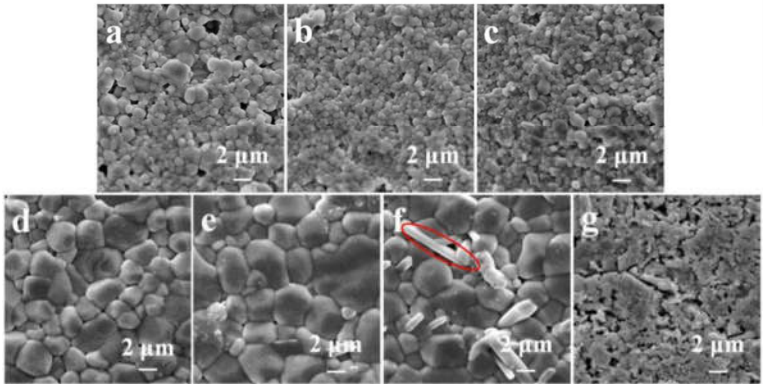

Figure 5. *SEM images of the $Ba(Zr_{0.1}Ti_{0.9})O_3$-based ceramics with different Li-Si-O contents: (a) 0 wt%; (b) 0.04 wt%; (c) 0.08 wt%; (d) 0.10 wt%; (e) 0.20 wt%; (f) 0.60 wt%; (g) 0.80wt%.*

Figure 5 shows the morphology of the $Ba(Zr_{0.1}Ti_{0.9})O_3$-based ceramics with different Li-Si-O contents. The relative densities of the samples with 0.0, 0.04, 0.08, 0.10, 0.20, 0.60, and 0.80 wt% Li-Si-O contents were 5.267, 5.402, 5.756, 5.909, 5.885, 5.834, and 5.813 g/cm^3, respectively. Thus, the density first increased and then decreased with increasing Li-Si-O content. The grain size gradually increased with increasing Li-Si-O content, and the grains became blurry as the Li-Si-O content reached 0.80 wt%. The Li-Si-O sintering agent shows great clearly influenced the densification behavior and sintering temperature. During sintering process, Li-Si-O melts and forms a liquid phase that spreads across the surface of the $Ba(Zr_{0.1}Ti_{0.9})O_3$ particles. The melting phase occupies regions with a higher energy configuration such as smaller grains and pores to reduce the total energy of the ceramic system [24]. During a subsequent stage of sintering, after the liquid layers touch and merge the grains rearrange, leading to a more compact structure as a result of the forces induced by the capillary liquid bridges among the small grains [25]. The effect of the wetting action of the liquid phase improves the efficiency of mass transfer, and permits a lower sintering temperature for the Li-Si-O-doped $Ba(Zr_{0.1}Ti_{0.9})O_3$ ceramics. The secondary phase that appeared at 0.60 wt% Li-Si-O (the red circles in Fig. 5f) as the increase of Li-Si-O content, which was consistent with the XRD results.

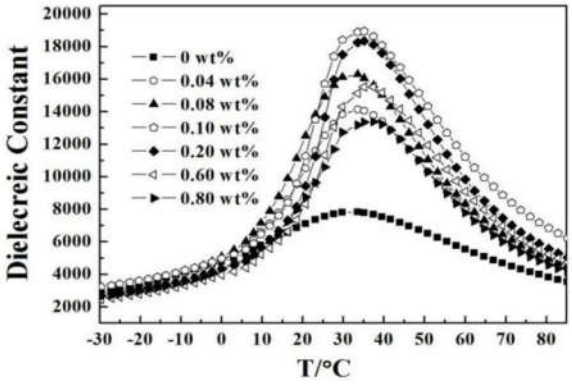

Figure 6. *Temperature dependence of the dielectric constant of $Ba(Zr_{0.1}Ti_{0.9})O_3$-based ceramics with different Li-Si-O contents.*

Table 2. *Main Properties of the $Ba(Zr_{0.1}Ti_{0.9})O_3$-based ceramics with different Li-Si-O contents. Abbreviations: tanδ, dielectric loss; ε_{max}, maximum dielectric constant; ε_r, room-temperature dielectric constant; Tc, Curie temperature; TCC, temperature-capacitance characteristic.*

Li-Si-O content (wt%)	Tanδ (25°C)	ε_{max}	ε_r(25°C)	Tc/°C	TCC (%)		
					-30°C	Tc	+85°C
0	0.05%	7818	7560	34	-58.70	3.41	-53.08
0.04	0.08%	14127	12527	34	-76.25	12.77	-65.18
0.08	0.09%	16289	14897	34	-79.78	9.34	-69.74
0.10	1.00%	18942	18897	35	-79.38	20.52	-60.33
0.20	1.10%	18348	17507	35	-80.18	34.28	-63.11
0.60	0.09%	15524	14315	37	-78.29	37.00	-69.78
0.80	0.08%	13392	9641	37	-75.08	26.39	-60.67

Figure 6 shows the temperature dependence of the dielectric constant of all the samples with different Li-Si-O contents over the temperature range from -30 °C to 85 °C. The main properties of these samples are listed in Table 2. The dielectric constant increased first and then decreased with increasing Li-Si-O content, reaching a maximum of 18942 at a Li-Si-O content of 0.10 wt%. This can be explained by the increasing densification of the ceramics after adding Li-Si-O, which also increased the dielectric constant. That constant then decreased as the Li-Si-O content increased further, which could be caused by the development of secondary phases at high Li-Si-O contents [26]. The most important result is that the temperature-capacitance characteristic (TCC) of the samples with a Li-Si-O content less than 0.20 wt% met the Y5V standards. The Li-Si-O content had no significant effect on the Curie temperature (Tc), although the ceramics exhibited a slight shift to a higher Curie temperature at high Li-Si-O wt%. On the one hand, the Li^{+} and Si^{4+} ions stay near the grain boundaries and rarely enter the lattice. On the other hand, the coarser grains of the ceramics produced at high Li-Si-O wt% and the appearance of a secondary phase with the added glass would decrease internal stresses among the grains, thereby increasing Tc [27]. In addition, the dielectric loss increased first and then decreased with increasing Li-Si-O content, which may relate to changes in the porosity of the ceramics.

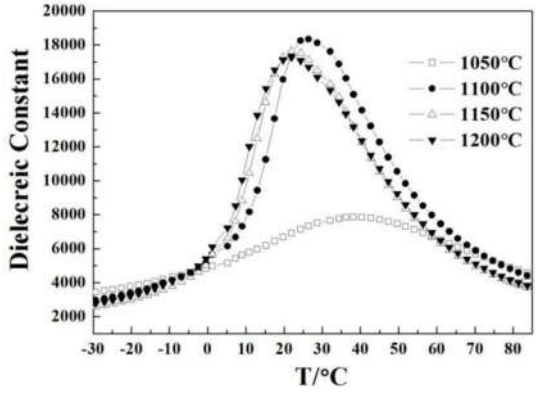

Figure 7. *Temperature dependence of the dielectric constant of the $Ba(Zr_{0.1}Ti_{0.9})O_3$-based ceramics with the same Li-Si-O content (0.10 wt%, added continuously) produced at different sintering temperatures.*

Figure 7 shows the temperature dependence of the dielectric constant of the $Ba(Zr_{0.1}Ti_{0.9})O_3$-based ceramics with the same Li-Si-O content (0.10 wt%) at different sintering temperatures. The dielectric constant of the ceramics increased first and then decreased with increasing sintering temperature, and the sintering temperature could be reduced to 1100 °C without decreasing the ceramic's performance. Thus, adding an appropriate Li-Si-O content can effectively reduce the sintering temperature and improve the dielectric properties of the $Ba(Zr_{0.1}Ti_{0.9})O_3$-based ceramics.

4. CONCLUSION

We studied the effect of how the Li-Si-O was added on the dielectric properties of the $Ba(Zr_{0.1}Ti_{0.9})O_3$-based ceramics. We found that the dielectric constant of the ceramics increased significantly when the Li-Si-O was added step by step, but degraded when it was added in one-step. The dielectric constant increased first and then decreased with increasing Li-Si-O content, and reached a maximum of 18942 at a Li-Si-O content of 0.10 wt%. The TCC of the samples with a Li-Si-O content less than 0.20 wt% met the Y5V standards. The Li-Si-O reduced the sintering temperature of the ceramics to 1100 °C, and the dielectric constant increased first and then decreased with increasing sintering temperature. Therefore, adding an appropriate amount of Li-Si-O step by step to the $Ba(Zr_{0.1}Ti_{0.9})O_3$-based ceramics can effectively improve their dielectric properties and reduce the sintering temperature.

ACKNOWLEDGEMENT

We thank the Shaanxi Provincial Department of Education Special Scientific Research Project (grant number 19JK0035); National Natural Science Foundation of China (grant number 21071115); Shaanxi Province Natural Science Foundation Research Project (grant number 2016JZ006); and Shaanxi Light Optoelectronics Material Co., Ltd (grant number 2015610002001920) for funding our research.

CONFLICT OF INTEREST

We declare that we have no conflict of interest.

REFERENCES

1. Kishi, H., Mizuno, Y., Chazono, H., "Base-metal electrode-multilayer ceramic capacitors: past, present and future Perspectives", *Jpn. J. Appl. Phys.,* 42 (2003) 1-15.
2. Kim, Y. K., Jung, Y. G., Sung, T. H., Kim, D. H., Paik, U., "Influence of burnout process on pore structure and burnout microstructure in $BaTiO_3$-based Y5V materials", *J. Mater. Process. Tech.,* 152 (2004) 276-283.
3. Zhang, X. H., Yue, Z. X., Peng, B., Xie, Z. K., Yuan, L. X., Zhang, J. L., Li, T., "Polarization response and thermally stimulated depolarization current of $BaTiO_3$\r$_3$\r-based Y5V ceramic multilayer capacitors", *J. Am. Ceram. Soc.,* 97 (2014) 2921-2927.
4. Hao, Y. N., Wang, X. H., Zhang, H., Zhang, Y. C., Li, L. T., "A novel approach to the preparation of a highly crystallized $BaTiO_3$ layer on Ni nanoparticles", *J. Am. Ceram., Soc.,* 96 (2013) 2696-2698.
5. Jean, J. H., Chang, C. R., "Effect of densification mismatch on camber development during cofiring of nickel-based multilayer ceramic capacitors", *J. Am. Ceram. Soc.,* 80 (1997) 2401-2406.
6. Kim, S. H., Koh, J. H., "Li-doped (Ba,Sr)TiO_3 thick film interdigital capacitors for microwave applications", *Microelectron. Eng.,* 86 (2009) 59-62.
7. Zhou, L. Q., Jiang, Z. H., Zhang, S. R., "Electrical Properties of $Sr_{0.7}Ba_{0.3}TiO_3$ Ceramics Doped with Nb_2O_5, $3Li_2O{\cdot}2SiO_2$, and Bi_2O_3", *J. Am. Ceram. Soc.,* 74 (11) (1991) 2925-2927.
8. Valant, M., Suvorov, D., Pullar, R. C., Sarma, K., Alford, N. M., "A mechanism for low-temperature sintering", *J. Eur. Ceram. Soc.,* 26 (2006) 2777-2783.
9. Maurya, D., Ahn, C. W., Zhang, S. J., Priya, S., "High dielectric composition in the system Sn-Modified (1-x)$BaTiO_3$-x$Ba(Cu_{1/3}Nb_{2/3})O_3$, x=0.025 for multilayer ceramic capacitors", *J. Am. Ceram. Soc.,* 93 (2010) 1225-1228.
10. Wang, Y. L., Li, L. T., Qi, J. Q., Gui, Z. L., "The effect of Sm_2O_3-dopant on the microstructure and dielectric properties of $BaZr_xTi_{1-x}O_3$ ceramics", *Ferroelectrics.,* 262 (2001) 233-238.
11. Wang, Y. L., Li, L. T., Qi, J. Q., Gui, Z. L., "Ferroelectric characteristics of ytterbium-doped barium zirconium titanate ceramics", *Ceram. Int.,* 28 (2002) 657-661.
12. Wang, Y., Cui, B., Zhang, L. L., Hu, Z. Y., Wang, Y. Y., "Phase composition, microstructure, and dielectric properties of dysprosium-doped $Ba(Zr_{0.1}Ti_{0.9})O_3$-based Y5V ceramics with high permittivity", *Ceram. Int.,* 40 (2014) 11681-11688.
13. 13.Fan, G. N., Huang, L. X., He, X. G., "Synthesis of singlecrystal $BaTiO_3$ nanoparticles via a one-step sol-precipitation route", *J. Cryst. Growth.,* 279 (2005) 489-493.
14. Boulos, M., Guillemet-Fritsch, S., Mathieu, F., Durand, B., Lebey, T., Bley, V., "Hydrothermal synthesis of nanosized $BaTiO_3$ powders and dielectric properties of corresponding ceramics", *Solid. State. Ionics.,* 176 (2005) 1301-1309.
15. Cernea, M., Monnereau, O., Llewellyn, P., Tortet, L., Galassi, C., "Sol-gel synthesis and characterization of Ce doped $BaTiO_3$", *J. Eur. Ceram. Soc.,* 26 (2006) 3241-3246.
16. Mohammad-Rezaei, R., Razmi, H., "Preparation and characterization of reduced graphene oxide doped in Sol-Gel derived silica for application in electrochemical double-layer capacitors", *Int. J. Nanosci. Nanotechnol.,* 12 (2016) 233-241.
17. Zhan, X. X., Cui, B., Xing, Y. L., Ma, R., Xie, Y., Chang, Z. G., Zhang F. X., "A novel process to synthesize high-k 'Y5V' nano-powder and ceramics", *Ceram. Int*., 38 (2012) 389-394.
18. Das, R., Pramanik, P., "Chemical synthesis of fine powder of lead magnesium niobate using niobium tartarate complex", *Mater. Lett.,* 46 (2000) 7-14.
19. Yamaga, M., Masui, Y., Kodama, N., "Temperature dependence of persistent phosphorescence in Eu^{2+}-doped Ba_3SiO_5", *Opt. Mater.,* 36 (2014) 1776-1780.
20. Zajc, I., Drofenik, M., "Preparation of $BaTiO_3$ PTCR ceramics by low temperature liquid sintering", *Key. Eng. Mater.,* 136 (1997) 1329-1332.
21. Hu, Q., Wang, T., Jin, L., Wei, X. Y., "Dielectric and energy storage properties of barium strontium titanate based glass-ceramics prepared by the sol-gel method", *J. Sol-Gel. Sci. Technol.,* 71 (2014) 522-529.

22. Qi, J. Q., Li, L. T., Li, W., "The influence of doping style on the grain growth of $BaTiO_3$ ceramics", *Mater. Sci. Eng. B.,* 99 (2003) 214-216.
23. Cui, X. M., He, Y., Liang, Z. Y., Zhang, H., Zhou, J., "Different microstructure BaO-B_2O_3-SiO_2 glass/ceramic composites depending on hightemperature wetting affinity", *Ceram. Int.,* 36 (2010) 1473-1478.
24. Liu, C., Zhang, H. W., Su, H., Zhou, T. C., Li, J., Chen, X., Miao, W. Z., Xie, L., Jia, L. J., "Low temperature sintering BBSZ glass modified $Li_2MgTi_3O_8$ microwave dielectric ceramics", *J. Alloys. Compd.,* 646 (2015) 1139-1142.
25. Wang, G., Jiang, J., Dou, Z., Zhang, F., Zhang, T., "Sintering behavior and microwave dielectric properties of $0.67CaTiO_3$-$0.33LaAlO_3$ ceramics modified by B_2O_3-Li_2O-Al_2O_3 and CeO_2", *Ceram. Int.,* 42 (2016) 11003-11009.
26. Ma, R., Cui, B., Wang, Y. J., Wang, S. Y., Wang, Y. Y., "The energy storage properties of fine-grained $Ba_{0.8}Sr_{0.2}Zr_{0.1}Ti_{0.9}O_3$ ceramics enhanced by MgO and ZnO-B_2O_3-SiO_2 coatings", *Mater. Res. Bull.,* 111 (2019) 311-319.
27. Zhai, J. W., Yao, X., Cheng, X. G., Zhang, L. Y., Chen, H., "Dielectric properties under dc-bias field of $Ba_{0.6}Sr_{0.4}TiO_3$ with various grain sizes", *Mater. Sci. Eng. B.,* 94 (2002) 164-169.